Journal of Heat and Mass Transfer Research 11 (2024), Serial Number 21, 15 – 32

Semnan University

Journal of Heat and Mass Transfer Research

Journal homepage: https://jhmtr.semnan.ac.ir

ISSN: 2383-3068

Review Article

Physical Overview of the Instability in Laminar Wall-Bounded Flows of Newtonian Fluids at Subcritical Reynolds Numbers

Hamed Mirzaee [a*], Goodarz Ahmadi [b], Roohollah Rafee [a], Farhad Talebi [a]

[a] *Faculty of Mechanical Engineering, Semnan University, Semnan, Iran*

[b] *Department of Mechanical and Aerospace Engineering, Clarkson University, Potsdam, NY, USA*

ARTICLE INFO

Article history:

Received: 2023-07-29

Revised: 2024-01-27

Accepted: 2024-01-28

Keywords:

Flow;

Instability;

Transition;

Perturbation;

Amplitude.

ABSTRACT

This paper reviews the latest findings on instability and subcritical transition to turbulence in wall-bounded flows (i.e., pipe Poiseuille flow, plane channel flow, and plane Couette flow). The main focus was on the early stage of transitional flow and the appearance of coherent structures. The scaling of threshold disturbance amplitude for the onset of natural transition was discussed. Generally, the scaling proved to be in the form of $A_c = O(Re^{\gamma})$ for Newtonian fluids where Re is the Reynolds number, $\gamma \leq -1$, and A_c is the critical perturbation amplitude. It was noted that exploration of perturbations like vortices, streaks, and traveling waves together with their amplitudes could clarify the instability and transition process. Hence, this paper focused on physical behavior and realizations of the transitional flow. Finally, a summary of consequential implications and some open issues for future works were presented and discussed.

1. Introduction

Gotthilf Hagen, a hydraulic and civil engineer, was the first to realize and think about the transition to turbulence in his study of pipe flow (Eckert [1]). Almost 30 years later, in 1883, Osborne Reynolds determined in his experiments that the Poiseuille flow in pipe remains stable to small disturbances up to the value of UD/ν equals 13000 in some experiments. This UD/ν was later called Reynolds number, Re, in 1908. Years later, Ekman [2] reached the value of 50000 utilizing Reynolds' authentic setup in more refined experiments. Thus, this type of flow was stable for Re >> 1 if he decreased the vibration of the experimental apparatus and disturbances of the incoming flow further. Observations of Pfenniger [3] and the linear stability analysis also admitted this is the case (e.g., see Kundu and Cohen [4]). It is noteworthy that Meseguer & Trefethen [5] showed that this flow remains linearly stable up to Re = 10^7. However, it is known that the pipe flow becomes unstable for certain small disturbances as the Reynolds number approaches 2000. Since 2000 >> 1 physically, this contradiction should be somehow addressed in fluid mechanics, and the minimum amplitude of disturbance for the onset of transition should be established.

Subcritical transition signifies that a fluid flow transitions to turbulence at a Reynolds number, which is much less than the prediction of linear stability theory (John et al. [6]). In other words, such a flow is nonlinearly unstable to the finite-

* **Corresponding author.**

E-mail address: h.mirzaee@alum.semnan.ac.ir ; h.mirzaee.mec@gmail.com

Cite this article as:

Mirzaee, H., Ahmadi, G., Rafee, R, Talebi, F., 2024. Physical Overview of the Instability in Laminar Wall-Bounded Flows of Newtonian Fluids at Subcritical Reynolds Numbers. *Journal of Heat and Mass Transfer Research*, 11(1), pp. 15 - 32.

https://doi.org/10.22075/JHMTR.2024.31381.1466

amplitude perturbation. For convenience, the first results of linear stability analysis for pipe Poiseuille flow, channel flow, and plane Couette flow of Newtonian fluids are listed in Table 1.

Table 1. Early studies on linear stability analysis for Newtonian fluids subject to small amplitude disturbances

Flow type	Wall type	Effective parameter(s)	Critical value(s)	Reference
Plane Couette	Rigid	Re	Re → ∞	Romanov [7]
Plane channel/Plane Poiseuille	Rigid	Re	Re = 5772	Orszag [8]
Pipe Poiseuille	Rigid	Re	Re → ∞	Davey & Drazin [9]

Using the linear stability theory, Orszag [8] obtained a critical Reynolds number of 5772 (based on centerline velocity and channel half-height) for the plane Poiseuille flow, whereas Herbert [10] computed the value of 2935 (based on the same definition of Reynolds number) using weakly non-linear stability theory. More importantly, Nishioka et al. [11] confirmed experimentally the theoretical value of 5772 by keeping the percentage of the background turbulence at about 0.05%. However, this flow becomes turbulent experimentally for Reynolds number of 1000 (with a sudden appearance of turbulent spots or bursts) when the background turbulence is not well controlled (see Patel & Head [12] and Schmid & Henningson [13]).

Incidentally, there is a stability theorem derived from the Reynolds-Orr energy equation, the energy method (Serrin [14]), for evaluating stability under finite amplitude disturbances. Accordingly, the predicted critical Reynolds number for the plane Poiseuille flow is 49.6 (Joseph and Carmi [15]), much less than the experimental value of 1000. Shahinpoor and Ahmadi [16] and Ahmadi [17] utilized the energy method for evaluating the stability criteria for the Cosserat and micropolar fluids under varying conditions.

The primary motivation for the present study was to review subcritical transitions in pipe flow, channel flow, and plane Couette flow and summarize the latest significant physical (empirical) and numerical findings concerning the transitional flow. The authors believed that this review article would be of interest to physicists, mathematicians, and engineers interested in the field of instability in fluid dynamics. Likewise, this review will complement a recent review paper (Mirzaee et al. [18]) which discusses the subcritical transition of viscoplastic and viscoelastic fluids in wall-bounded flows.

This study mainly reviews the literature concerning the subcritical transition since 2002 from the physical perspective with some references to seminal older papers. Readers can refer to the monograph by Yalgom and Frisch [19] on unstable and transitional Newtonian flows for a comprehensive review of the literature before 2002. It should be stressed that this review article does not include the transition from the dynamical systems viewpoint and prominent subjects like "directed percolation," "edge states," and "optimal pattern of transition" that were reviewed by Manneville [20].

The paper is organized as follows. Section 1 introduces the historical and early works concerning the transition in wall-bounded shear flows. Next, the relevant equations are expressed in section 2. Sections 3, 4, and 5 are devoted to the pipe Poiseuille flow, the plane Poiseuille flow, and the Plane Couette flow, respectively. Finally, concluding remarks and some open issues for future works are mentioned in the Conclusion section.

2. Governing Equations and Disturbance Amplitude Definition

In this section, the transition of Newtonian fluids is discussed and is divided in terms of flow type, although some studies investigate two flow types. The continuity and the Navier-Stokes equation are given as:

$$\nabla \cdot \vec{u} = 0 \tag{1}$$

$$\rho \frac{\partial \vec{u}}{\partial t} + \rho(\vec{u} \cdot \nabla \vec{u}) = -\nabla p + \mu \nabla^2 \vec{u} \tag{2}$$

where $\vec{u}$ is the velocity vector, p is the pressure, and μ is the dynamic viscosity.

The perturbed velocity and pressure fields are written as:

$$\vec{u} = \vec{U} + \overrightarrow{u'}, \qquad p = P + p' \tag{3}$$

Here, the capital letters denote the basic state, and the letters with prime denote the perturbation. Note that the Reynolds number is defined as $Re = \frac{\rho U_0 L_0}{\mu}$, where U_0 is the characteristic velocity and L_0 is the characteristic length. Typical velocities for definitions of Re for pipe Poiseuille flow, plane Poiseuille flow, and plane Couette flow, respectively, are the mean velocity, the centerline velocity, and the upper (i.e., moving) wall velocity. Typical lengths for definitions of Re are the diameter for the pipe Poiseuille flow, the half-channel height for the plane Poiseuille flow, and the channel height for the plane Couette flow. As for the plane Couette flow, if the upper and lower walls are both moving at the same velocity in opposite directions, the typical length for defining the Re is the half-channel height (Kuwabara [21]).

The instantaneous amplitude of perturbation velocity is defined as (Chapman [22]):

$$\left|\overrightarrow{u'}\right| = E^{1/2} = \left(\frac{1}{2V}\int \left(u'^2 + v'^2 + w'^2\right) dV\right)^{1/2} \quad (4)$$

where E is the perturbation kinetic energy, and V is the fluid volume.

Moreover, the relative or non-dimensional perturbation velocity is given by:

$$\left|\overrightarrow{u'}\right|^* = \frac{\left|\overrightarrow{u'}\right|}{U_0} \quad (5)$$

Eq. (5) can be used for the external disturbance imposed on the flow through a hole/slot or holes/slots on the wall, with the numerator treated as the average disturbance velocity over the hole or slot surface area.

3. Pipe Poiseuille Flow

3.1. Phenomenology of Transition and Critical Reynolds Numbers

In this subsection, the mechanisms associated with the unstable and transitional flows are introduced. Here, three distinct critical Reynolds numbers are considered. The first one is the global critical Re which means the critical Re below which the instability cannot happen regardless of the magnitude of the perturbation amplitude. The second one is the transitional Re which denotes the lowest critical Re for the onset of natural transition. The third one is the critical Re for the start of instability which refers to the lowest Re for an exponentially growing small-amplitude perturbation (Davies and White [23]; Meksyn and Stuart [24]; Stuart [25]; Tillmark and Alfredsson [26]). Among these critical Reynolds numbers, the first one is debatable, and there are no unanimous values of global critical Reynolds numbers for the pipe Poiseuille flow and plane Poiseuille flow (see Schmid & Henningson [13]).

Boberg & Brosa [27] numerically showed that small disturbances could induce stronger disturbances in pipe flow. This process allowed the onset of the chaotic behavior in linearly stable flows. They were the first to notice that disturbance can grow significantly before decay.

Trefethen et al. [28] used the idea of Boberg & Brosa [27] to present a model (i.e., a dynamical system) to consider the feedback of nonlinear terms on the unsteady solution of a system of differential equations. It should be noted that transient growth of the perturbation amplitude leads to the transition. They determined that the threshold amplitude of order Re^{γ} in which $\gamma < -1$ leads to the transition. It is noteworthy that the Orr-Sommerfeld (O-S) equation (which is an eigenvalue problem) is obtained by linearizing the Navier-Stokes equations. Moreover, its adjoint equation is obtained by the inner product by the complex conjugate of the eigenfunction and integration by part. The O-S differential operator (L_{OS}) is non-normal in the sense that the multiplication of the operator and its adjoint operator (L_{OS}^{+}) is not commutative ($L_{OS}L_{OS}^{+} \neq L_{OS}^{+}L_{OS}$). For this reason, the O-S eigenfunctions are not orthogonal to each other (Schmid & Henningson [13]). The non-normality of the O-S operator affects the dynamics of small-amplitude three-dimensional disturbances. That is, the small-amplitude perturbations may be transiently amplified by factors of 10^3 to 10^4, although all eigenfunctions eventually decay (Trefethen et al. [28]). In addition, the physical mechanism for the transient growth is the lift-up effect.

The mechanism of streak formation, known as the lift-up effect, is shown schematically in Figure 1. As seen, the streamwise vortices are capable of lifting the low-speed streak near the wall into the faster region (Landahl [29]). Likewise, Davidson [30] remarked that near the wall in a turbulent boundary layer, many counter-rotating streamwise vortices move the fluid toward and away from the wall. Further, a pair of streamwise vortices are foot-points of two legs of a hairpin vortex (see Hinze [31]).

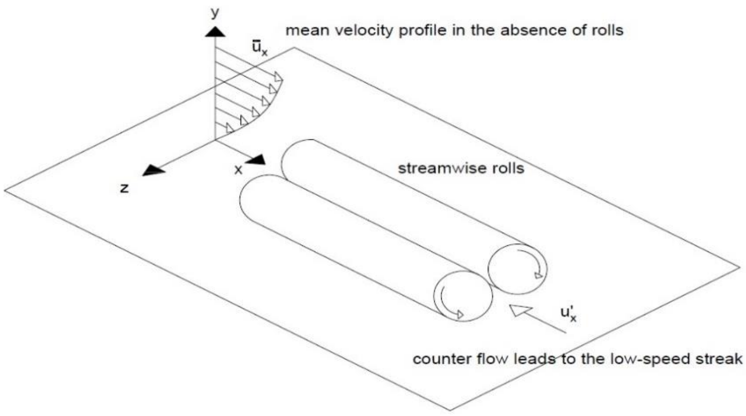

Fig. 1. Lifting low-speed streak near the wall by streamwise vortices (Davidson [30]).

Schmid and Henningson [32] numerically demonstrated that the maximum energy amplification of initial disturbances in laminar pipe flow occurs for those with zero streamwise wavenumber and fundamental azimuthal wavenumber. Figure 2 shows the transient growth of the total energy of disturbances against time for two streamwise wavenumbers of α = 0.1 and α = 1. The summary of maximum energy growth for wall-bounded shear flows was given by Schmid & Henningson [13] (see Table 4.1 of their work). The input-output analysis (initially utilized in the control theory) of linearized Navier-Stokes equations can be utilized to calculate the transient energy growth. The varying body forces or nonlinear terms are considered inputs, and the resulting velocity components are deemed as outputs. Furthermore, the "amplification" or "gain" of a system describes the relative size of an output to an input (Jovanovic [33]). Farrell and Ioannou [34] and Bamieh and Dahleh [35] studied transient amplification due to stochastic background noise using this methodology. Recently, Jovanovic [33] reviewed the application of the input-output analysis for the amplification of deterministic and stochastic disturbances and the identification of unstable flow structures.

Darbyshire and Mullin [36] reported the experimental study of transitional pipe flow. The disturbance was created using a single jet or multiple jets in the fully developed region. They could produce a laminar flow up to Re = 9900. It was shown that a critical disturbance amplitude is required to start transition at a certain Re, and it is a slowly decreasing function of Reynolds number for Re ≥ 2100. Moreover, a sustained transition was not accessible for Re < 1760, irrespective of the disturbance amplitude.

Fedotov et al. [37] investigated the effect of adding stochastic noise to the Trefethen et al. [28] proposed model. They stated that random fluctuations might cause the subcritical transition in fluid flow.

Bergstrom [38] analytically studied the transient growth of streamwise-independent disturbances under the effect of the Earth's rotation. He found that the Coriolis force can decrease the transient amplification by one-third compared with the case it is not included.

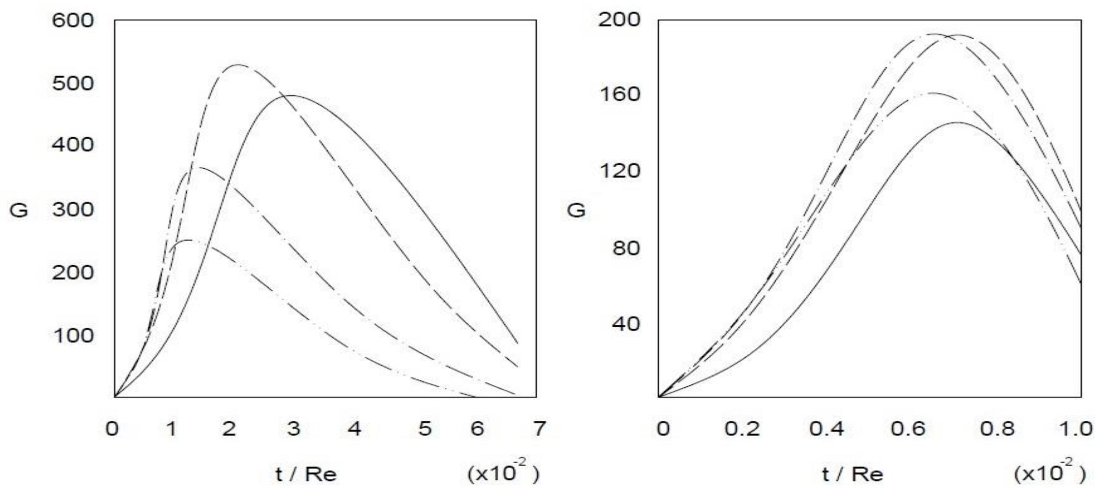

Fig. 2. Transient growth of the kinetic energy of disturbances in pipe Poiseuille flow for Re = 3000. For the left and right graphs, α = 0.1 and α = 1, respectively. Here, the solid line is related to n = 1, the dashed line is n = 2, the dash-dot line is n = 3, and the dash-double-dot line is n = 4. Note that $G(t) = E(t)/E_0$ is the growth function with E_0 being the initial total kinetic energy of disturbances, α is the streamwise wavenumber, and n is the azimuthal wave number (Schmid and Henningson [32]).

Faisst and Eckhardt [39], simultaneously with Wedin and Kerswell [40], identified and presented traveling waves downstream in pipe flow as precursors to transition. They pointed out that these traveling waves produce low-speed streaks toward the center and high-speed streaks near the wall. It should be noted that a single upstream vortex pair cannot produce coherent symmetric waves. Figure 3 illustrates the traveling wave at a cross-section with azimuthal wavenumbers of 2, 3, 4, and 5. The lowest critical Re was 1250, related to the 3 pairs of vortices. It is noteworthy that these traveling wave solutions are based on the self-sustaining process (SSP) suggested by Waleffe [41]. SSP means that the cycle of streamwise rolls, streamwise streaks, and three-dimensional waves preserves each other against relaminarization by viscosity. In other words, this process comprises three stages: formation of streaks by the streamwise vortices, breakdown of streaks due to the inflectional instability of the streaks, and regeneration of streamwise vortices (Hamilton et al. [42]). It is well worth mentioning that the first stage is common between the nonlinear SSP and the linear transient growth (Waleffe [41]). However, Waleffe [43], using a realistic mathematical model of a nonlinear system of coupled ordinary differential equations for the plane Couette flow, proved that the transient growth does not directly trigger the transition. Moreover, Hof et al. [44] observed these traveling waves experimentally. Accordingly, the traveling wave has two-fold or three-fold rotational symmetry inside a puff (i.e., the localized perturbation structure seen at Re < 2800), while it has a combination of two-fold and four-fold rotational symmetries or a combination of three-fold and six-fold rotational symmetries inside a slug (i.e., the localized perturbation structure seen at Re ≥ 3000).

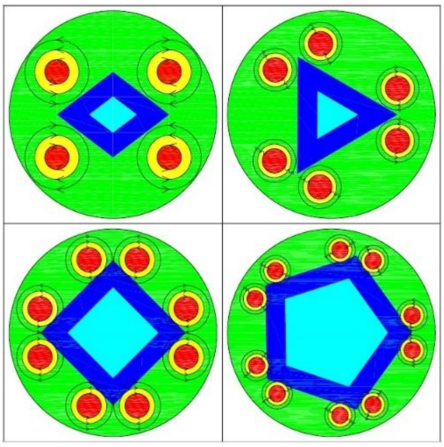

Fig. 3. Space-averaged velocity vectors and contours of axial velocities illustrate the streamwise vortices and locations of streamwise streaks at the cross-section of a pipe, respectively. High-speed axial streaks are near the walls, and low-speed ones are near the centers (Faisst and Eckhardt [39]).

Mellibovsky and Meseguer [45] numerically explored the streak breakdown route to turbulence. They introduced both 2-D and 3-D perturbations at the pipe inlet simultaneously. By monitoring the temporal development of the kinetic energy of streaks, they classified all their simulation runs into three groups: laminar, turbulent, and relaminarized. They suggested that the oblique transition scenario differed from the streak breakdown scenario.

Mullin and Peixinho [46] performed an experimental investigation on transition in pipe flow. They observed that upstream disordered flow could not persist for Re ≤ 1750 for perturbation amplitude of 0.01 and 0.1. The Re = 1750 was deemed as the global stability criterion. Another point about this experiment is that the scaling law of Re-1, previously reported for the required amplitude to start the transition, did not hold for Re < 1750.

Eckhardt et al. [47] discussed transition features in pipe flow. They commented that flow patterns are not likely to be the same as the exact traveling solutions found by Faisst and Eckhardt together with Wedin and Kerswell in 2004. However, the appearance of high and low-speed streaks and vortex rolls (being azimuthally periodic) help detect the flow state. Their key finding was that the coherent flow structures (i.e., streamwise vortices and streaks) increase with the Reynolds number rise.

Nishi et al. [48] developed a test facility to investigate the transition to turbulence in pipe flow. It was shown that non-dimensional obstacle height for triggering transition varies with Reynolds number as $Re^{-1/2}$. Moreover, when the Reynolds number was reduced below Re = 1940, the turbulent patches could not be sustained, and the flow was relaminarized.

Loh & Blackburn [49] examined the linear instability of steady flow through an axially corrugated pipe. They noted that the separation bubble in the corrugation region did not cause instability. Moreover, it was argued that non-axisymmetric vortices are less stable than axisymmetric ones, and the critical Reynolds number was reported to be 1971, commensurate with the azimuthal wavenumber of 3. This study was in line with instability analysis in 2-D corrugated channel flow performed by Floryan [50].

Tasaka et al. [51] investigated the transitional pipe flow. It was shown that the non-turbulent transients decay before 100D (D is the diameter). By comparing the probability of observation of puff or slugs, it was mentioned that transition is sharp and dependence of the probabilities on the disturbance amplitude is non-monotonic. Thus, ascribing certain values to threshold amplitudes is not useful.

Avila et al. [52] presented an approach for finding the exact critical Reynolds number for the onset of sustained turbulence in the pipe flow using experiment and direct numerical simulation. It was shown that the intersection of puff (i.e., the localized perturbation structure seen at Re < 2800) mean lifetime and mean splitting time equals 2020±10. Importantly, this study revealed that spatial proliferation of chaotic fluid motions underlies turbulence, which is at odds with the classical view that turbulence is the result of the temporal complexity of fluid motion.

Mullin [53] did a comprehensive review of the transition process in pipe flow. He stated that the minimum length of the domain should be 30D if numerical calculations are to be performed for low values of Re, i.e., 2000 < Re < 3000, to consider the puff. It was found that for Re > 2000, a smaller amplitude disturbance causes a transition in the entry flow, whereas a larger amplitude is needed for the fully developed flow. He also emphasized that the transition to turbulence is abrupt for Re > 3000 but unclear for 1800 < Re < 3000.

Krauss et al. [54] performed an experimental study of transition in pipe flow for 1500 < Re < 2900. It was found that the probability of occurrence of a single puff is unity when Re roughly equals 2200, whereas that of other structures, like a single slug (i.e., the localized perturbation structure seen at Re ≥ 3000), is always less than one.

Trip et al. [55] investigated the transition of pulsatile pipe flows experimentally. They used turbulence level as a metric. Accordingly, transition arises in the range of Re = 2250 to Re=3000. The Womersley number, characterizing the pulsatile nature of flow, is defined as $Wo = R\sqrt{(2\pi f/\nu)}$ where R is the pipe radius, f is the pulse wave frequency and ν is kinematic viscosity. They suggested that for the typical range of Womersley numbers (10<Wo<25), pulsatile effects does not play an important role, and the transitional flow was controlled by the mean Reynolds number.

He & Seddighi [56] investigated the transient channel flow in three stages of pretransition, transition, and fully turbulent flows by direct numerical simulation. They noted elongated streamwise streaks, being stable during the pre-transition phase, and localized turbulent spots during the transition phase. Furthermore, the perturbation kinetic energy and root-mean-square streamwise velocity fluctuations grow transiently, whereas other root-mean-square velocity fluctuations remain almost unchanged in the transition stage.

Wu et al. [57] demonstrate that the breakdown of laminar flow in the pipe is not abrupt and happens by a series of events. They introduced inflow localized disturbance in the form of a ring, and laminar flow was maintained below Re = 8000. Further, it was argued that the energy norm of perturbation grows exponentially rather than algebraically.

Hellstorm et al. [58] investigated the transition in pipe flow using the particle image velocimetry method at Re = 3440. They divided the transitional flow into two regions. One was a pseudo-laminar region occupied by azimuthally traveling waves, and the other was turbulent slugs.

Novopashin et al. [59] devised an experiment to assess the critical Reynolds number for real gas flow inside a tube. They found that by augmenting the inlet pressure, the critical Re reduces. They added that the second virial coefficient of real gas (that changes with temperature) affects the transition.

Wu et al. [60] studied transitional pipe flow via direct numerical simulation. Based on their findings, turbulent spots contain reverse hairpin vortices near the wall and forward hairpin vortices in the core region. They commented that this dual composition might be a common feature regardless of the shape or mode of upstream inlet disturbances. Further, the number density of reverse hairpin vortices was quantified.

Cerbus and Mullin [61] carried out quench experiments on transitional pipe flow. They considered two driving techniques, i.e., constant pressure gradient (CPG) and constant mass flux (CMF). By measuring the turbulent fraction quantity, it was shown that transition begins at Re = 1750 for CMF and Re = 2040 for CPG. Thus, it was concluded that these flows are dynamically similar but they have different critical Reynolds numbers.

Zhou [62] reviews available theoretical and statistical approaches for turbulence research. He stated that turbulence theorists should correlate the data obtained from experiments and computations to develop a standard model for further research.

Ricco & Alvarenga [63] dealt with the growth of three-dimensional perturbation entrained in the entrance region of a pipe. The initial disturbances were introduced in the form of stream-wise vortices and streaks at the pipe mouth. Accordingly, decreasing frequency and streamwise wavenumber intensify the transient growth. It was found that an azimuthal wavelength of 2.09 causes the most energetic growth.

Hattori et al. [64] performed experiments on natural transition in pipe flow. Accordingly, the onset transition did not depend on the pipe length-to-diameter ratio. The transitional flow states were arranged in five groups, i.e., laminar, transition I, II, and III, and turbulent, corresponding to the Reynolds numbers 1200, 2300, 7000, and 12000, respectively. Notably, the Reynolds number of 1200 agreed with the critical Reynolds number of 1250 for the emergence of traveling waves solution found by Faisst & Eckhardt [39].

Avila et al. [65] reviewed the pipe flow transition as a good prototype for other wall-bounded flows. They compared two approaches for determining the critical Reynolds number; a direct approach used by Reynolds and an indirect one. In the second approach, the critical Reynolds number is the point where the decay timescale of isolated puffs equals the splitting timescale. This critical value is Re = 2040±10. They remarked that the scaling exponent for the critical point needs additional studies.

3.2. Scaling and Coherent Flow Structure

In this subsection, the scalings of perturbation amplitude for the onset of instability in pipe Poiseuille flow and some relevant coherent flow structures are mentioned. It is noteworthy that the coherent structures are signs of instability and transition to turbulence. Coherent flow structures are flow patterns or flow topologies that are identifiable and persistent for some periods of time and appear almost in the same form (Panton [66]; Davidson [30]). These structures can be identified by experiments of flow visualization, direct numerical simulation, and stability analysis. The most commonly observed coherent structure is the hairpin vortices in the turbulent boundary layer (Davidson [67]). Flow visualizations of Kline et al. [68] illustrated the coherent streaky structures (i.e., the streak formation and breakdown processes) in the turbulent boundary later. It can be said that the coherent flow structures include vortex, streak, traveling wave, localized perturbation, etc. In addition, some other structures are available in the unstable natural heat convection. The discrete cells of rhombic pattern are the coherent structure of the secondary instability of natural convection (see Hossain and Floryan [69]). Also, the puff and slug (localized perturbations) are the well-known coherent structures observed in the transitional pipe flow (Mullin [53]). Interestingly, James Thomson, a British engineer and physicist, was probably the first person who identified a coherent flow pattern in liquids at the onset of instability in 1882 (see Chandrasekhar [70]).

Draad et al. [71] set up a pipe-flow facility to experimentally find the critical disturbance velocity leading to the transition. They maintained a laminar flow up to Re = 60000 and a fully-developed laminar flow up to Re = 14300. The disturbance was introduced from a slit over the perimeter of the pipe wall. It followed from the observation at 100D downstream of the disturbing location that the critical disturbance velocity $v^*_{i,c}$ scales with Re^{-1} for $\alpha^* \geq 2$, with $Re^{-2/3}$ for $\alpha^* \leq 0.5$. Here, α^* is a non-dimensional axial wavenumber (see Fig. 4).

Hof et al. [72] experimented with a piston-driven flow in a very long pipe with a length-to-diameter ratio of 768. They probed both temporal and spatial initial disturbances. Laminar flow was obtained for Re < 18000. Furthermore, they conjectured that the perturbation amplitude needed for transition varies as Re-1.

Meseguer [73] analyzed the stability of pipe flow, focusing on the streak breakdown process. He considered 2-D and 3-D initial perturbations collectively. Accordingly, the required amplitude for destabilization is of the order of $Re^{-3/2}$. He commented that the scaling law by Chapman [22] is useful for asymptotic ranges of Reynolds numbers (i.e., Re → ∞) but unsuitable for moderately high Reynolds numbers.

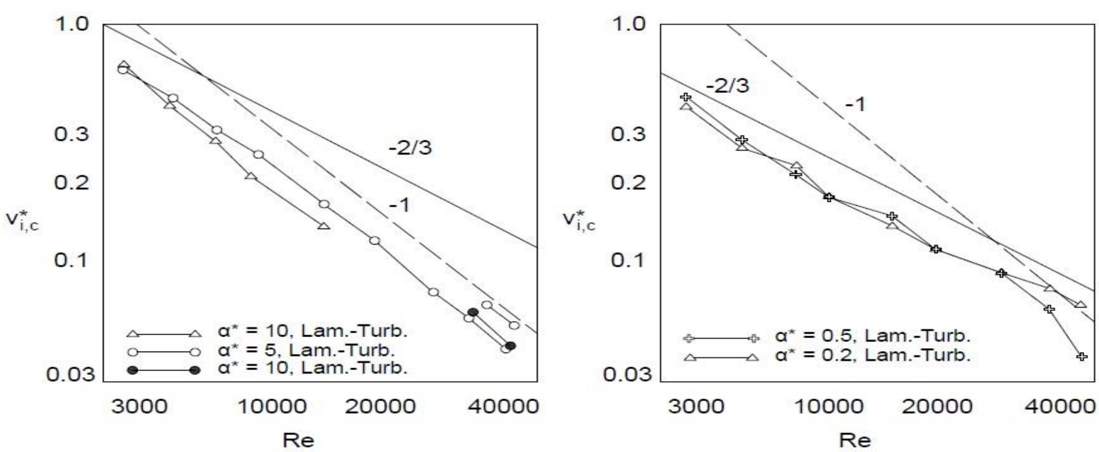

Fig. 4. The threshold perturbation velocity vs. Reynolds number for large (left panel) and small (right panel) wavenumbers (Draad et al. [71]).

Mellibovsky and Meseguer [74] numerically explored the subcritical transition of pipe flow through the streak breakdown scenario for Reynolds numbers in the range of 2.5×10^3 to 1.26×10^4. They consider a medium pipe length (20 radii) with 1, 2, and 3 pairs of streamwise vortices. They argued that the streak breakdown process is the primary cause of the transition to turbulence. It should be noted that the streak breakdown means that 3-D small waves destabilize and break 2-D streamwise streaks and produce turbulence. The minimum amplitude ($A = Re^{\gamma}$) was found to vary as $Re^{-1.47}$, $Re^{-1.1}$, and Re^{-1} for single, double, and triple pairs of streamwise vortices, respectively.

Ben-Dov and Cohen [75] numerically examined the destabilizing effects of non-axisymmetric distortion in pipe Poiseuille flow. Due to the bifurcation of the solution, two minima co-exist for initial energy or amplitude of distortion for triggering the transition. One was located near the wall, and the other was localized near the centerline. Accordingly, the minimal amplitude is scaled with Re^{-1} and is approximately equal to 20/Re.

Peixinho and Mullin [76] studied the finite-amplitude perturbation in pipe flow. They used a single normal jet, six azimuthal jets, and push-push disturbances. It was found that threshold amplitude concerning one jet and multiple jets scale with Re-1, whereas the amplitude of push-pull disturbance varies as $Re^{-1.3}$ or $Re^{-1.5}$. Accordingly, the configuration of jets did not alter the scaling law.

Mellibovsky and Meseguer [77] numerically explored pipe flow transition under impulsive perturbations. Trying to simulate the experiment of Hof et al. [72], it was evidenced that for Re = 4000 to 14000, the threshold amplitude is of $O(Re^{-1})$. However, there were large discrepancies for Re ≤ 2800. They ascribed this to the deviations of nominal and actual Reynolds number definitions.

Mellibovsky and Meseguer [78] postulated that the minimum amplitude for triggering the transition in pipe flow decreases as $Re^{-3/2}$ and Re^{-1} for initial non-axisymmetric and time-dependent impulsive disturbances, respectively. It should be noted that the first scaling was found for one pair of streamwise vortices, and the second one was found for six pairs of streamwise vortices due to the number and distance of injection slits around the perimeter of the pipe.

Tao [79] presented a theoretical model for the prediction of the instability of flow through a rough pipe. He reasoned that the roughness shape factor ($S = n\varepsilon$ with n being the axial wavenumber of the roughness) instead of roughness amplitude (ε) could characterize the critical condition. Therefore, the threshold shape factor scales like Re^{-2}. This model was consistent with the experimental data of Nikuradse [80], especially in the transitionally rough region. Note that the roughness mean height is proportional to the roughness mean amplitude (Schlichting and Gersten [81]). Thus, one can derive an experimental scaling for the critical roughness amplitude according to the well-known Colebrook formula [82] in the transitionally rough region as $f^{0.5}\varepsilon = O(Re^{-1})$ with f being the Darcy friction factor. In addition, the author suggested the coherent structure as in Fig. 5 for the unstable flow.

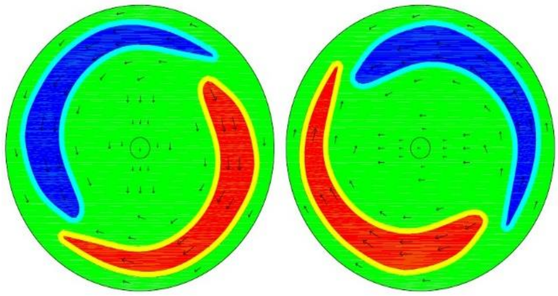

Fig. 5. The color contour of disturbing axial velocity shows a pair of regions with high or low axial velocity, and the vector plot shows a pair of streamwise vortices close to the pipe wall. The left Panel lags behind the right panel by half axial wavelength (Tao [79]).

Cerbus et al. [83] revisited the experimental work of Wygnanski & Champagne [84], trying to compare transitional pipe flow with puffs or slugs with fully turbulent pipe flow. They noted that the flow inside the slugs is fully developed. Likewise, slug flow and fully turbulent flow are indistinguishable at the same Reynolds number. Incidentally, the rich dependence of peak streamwise fluctuating velocity on the Reynolds number was demonstrated. Figure 6 demonstrates a single turbulent slug traveling and expanding downstream.

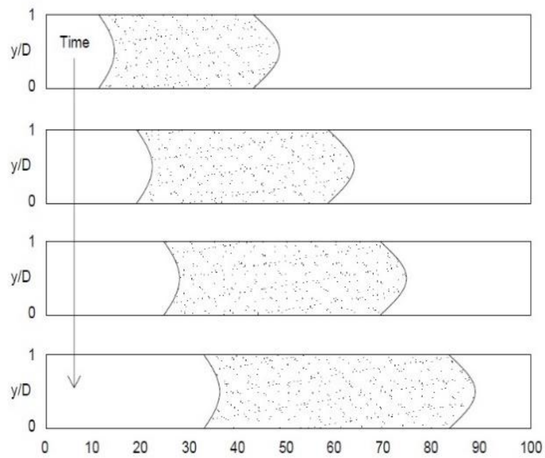

Fig. 6. A turbulent slug traveling downstream during the transition in a pipe flow (Cerbus et al. [83]).

Ozcakir et al. [85] analyzed the linear instability of laminar pipe flow along with wavy transpiration on the wall for 1000 < Re < 50000. They presented the neutral stability curve in terms of scaled transpiration amplitude (Λ) versus azimuthal wavenumber (N). Accordingly, the unstable mode corresponds to $N = 1$ when $\beta < \sqrt{2}$ and $N \approx [(3/2)\beta^2]^{1/3}$ for large N. Here, β represents the axial transpiration wavenumber. It was found that the drag decreases with augmenting β, the maximum being at $N = 2$ and $\beta = 1$.

4. Plane Poiseuille Flow

4.1. Phenomenology of Transition and Critical Reynolds Numbers

The mechanisms associated with traveling wave instability like the lift-up effect and the streak breakdown process (mentioned in subsection 3.1) can be seen in the plane Poiseuille flow. In this subsection, the subcritical instability of the plane Poiseuille flow, together with the different critical Reynolds numbers are discussed. It is noteworthy that Davies and White [23] performed experiments on channel flow with the width-to-depth ratio ranging from 40 to 160. Noticeably, they expressed Re = 1000 for the transitional Re. Further, they propounded that the global critical Re lies in the interval of 100 < Re < 1000. By direct numerical simulation, Orszag and Kells [86] established Re = 500 as the global critical Re if the flow is subject to three-dimensional disturbances.

Reddy et al. [87] compared the lowest threshold amplitude for the onset of transition in plane Poiseuille flow due to different initial disturbances at a subcritical Reynolds number. They found minimal energy for stream-wise and oblique vortices was by a factor of 100 lower than that for Tollmien-Schlichting waves and by a factor of 10 lower than that for two-dimensional optimal disturbance. An analogous study on energy amplification using the input-output analysis was carried out by Jovanović and Bamieh [88].

Biau and Bottaro [89] pointed out that in most bounded flows, transient growth and exponential instability growth due to small noises in experiments cause transition concurrently. Moreover, their results for energy growth differ significantly from those of Schmid et al. [90].

Zienicke and Krasnov [91] studied the boundary between stability and instability of electrically conducting fluid in a channel flow. They envisaged the streak breakdown phenomenon for predicting transition. They determined the minimal amplitudes of 0.01 and 0.0001, respectively, for 2-D and 3-D perturbations at the Re = 350. Furthermore, the size of the perturbation decreased by a factor of 0.001 when the Reynolds number varied from 350 to 1000.

Cohen et al. [92] numerically and experimentally assessed the instability and transition in pipe and channel flows. They asserted that the scaling laws of Chapman [22] and Hof et al. [72] are precise and that Re = 2000 is the critical Reynolds number for pipe flow with a finite-amplitude axisymmetric distortion.

Floryan and Floryan [93] considered the flow instability in a diverging-converging channel. It was discussed that the variation of the channel geometry could destabilize the fluid flow. Based on this study, the global critical Reynolds number for vortex instability decreases more rapidly than that for traveling wave instability with an increment in disturbance amplitude (S). It was suggested that when S is less than 0.0065, the traveling wave instability appears first, but for higher values of S, the vortex instability appears first.

The importance of transient growth in subcritical transition was discussed earlier. However, Kaminski et al. [94] used direct numerical simulations and showed that the transient growth of initial perturbation might be enough to give rise to transition in linearly stable stratified flow, e.g., in a channel. In other words, this growth can make the gradient Richardson number reach 0.25 in the flow field.

Roy et al. [95] assessed the transition in a parallel plate channel flow using direct numerical simulation based on the lattice-Boltzmann method. They placed a small amplitude surface roughness in the middle of the lower wall. It was illustrated that the effect of roughness on the onset of transition is less than that of disturbed inlet conditions, the critical Reynolds number being 2400 for the former and 1400 for the latter. Moreover, roughness induced gradual transition compared to inlet disturbances.

Sun and Hemati [96] studied the suppression of subcritical transition in plane Poiseuille flow through direct numerical simulation. It was argued and displayed that small-amplitude disturbance amplified much greater than finite-amplitude one. In fact, the nonlinearity in the flow hindered the transient energy amplification of disturbance. Intriguingly, it was found that the wall actuation (i.e., suction and blowing) as a control strategy could increase the threshold energy nearly by a factor of O(10).

Ren et al. [97] investigated the linear stability of highly non-ideal fluids (i.e., supercritical carbon dioxide gas) in the Plane Poiseuille flow. Both walls were at the same temperature (T_w), and the T_{pc} = 307.7 Kelvin was deemed the pseudo-critical temperature. Three cases of subcritical (T_w = 290 K), transcritical (T_w = 300 K), and supercritical (T_w = 310 K) for both ideal and non-ideal gases were evaluated. The zero Eckert number (Ec) corresponded to the isothermal flow. Increasing the Eckert number makes the ideal gas flow more stable (Rec > 5772) for the three cases. For the non-ideal gas, the flow becomes more unstable (Re < 5772) for the first and second cases but more stable for the third. Also, the maximum perturbation growth was seen at $\alpha = 0$ and $2 \leq \beta \leq 2.1$ with α being streamwise wavenumber and β being the spanwise wavenumber.

Khan et al. [98] used the threshold perturbation amplitude reported by Hof et al. [72] and direct numerical simulation to analyze transition flow dynamics in a square duct. They introduced an initial streamwise streak in the inlet. By comparing transition and turbulent kinetic energy spectra, it was unveiled that energy of inertial range in the transition region varies more than the turbulent region and scales with k^{-2}, k is the wavenumber.

Liu et al. [99], using the structured input-output analysis and including the nonlinearity, illustrated that optimal perturbation leading to the largest energy growth vanishes at the channel center, whereas, excluding the nonlinearity, the optimal perturbation peaks at the channel center.

4.2. Scaling and Coherent Flow Structure

In this subsection, the scalings of perturbation amplitude for onset of instability in plane Poiseuille flow, and an experimental coherent flow structure are mentioned. It is stressed that the coherent structures are signs of instability and transition to turbulence.

Lundbladh et al. [100] numerically examined the threshold amplitude for beginning the subcritical transition in channel flows. It was found that the amplitude scales as $Re^{-7/4}$ for Reynolds number in the range of 1500 to 5000.

Chapman [22] used asymptotic analysis (i.e., WKB theory) and showed that the amplitude of order $Re^{-3/2}$ and $Re^{-5/4}$ for streamwise and oblique perturbations initiates transition in the plane Poiseuille flow. Moreover, he stated that the initial wall-normal perturbation velocity of order ε makes the wall-normal perturbation vorticity of order εRe.

Philip et al. [101] set up an air-channel facility to validate the theoretical scaling law of Chapman [22] concerning the necessary disturbance amplitude for initiating the subcritical transition in channel flow. They achieved $v_0 = O(Re^{-1.53})$, agreeing with $v_0 = O(Re^{-1.5})$ derived by Chapman [22]. Note that v_0 stands for the normal disturbance velocity, and the length of the experimental channel was much less than the theoretical length considered. Figure 7 discloses the advent of streamwise vortices before the transition and hairpin vortices after transition in a channel flow.

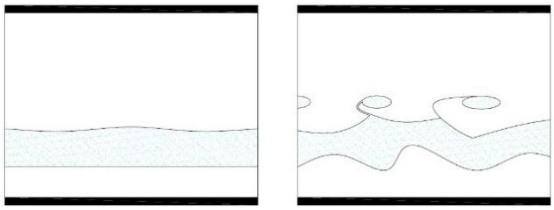

Fig. 7. Visualization of (a) a pair of streamwise vortices before the transition and (b) hairpin vortices after the transition in a channel. Note that the direction of the flow is from the left to the right, and the upper and lower boundaries are the channel walls (Philip et al. [101]).

Lemoult et al. [102] presented an experiment on the transition to turbulence in 2-D channel flow. They used the deformation of the mean velocity profile rather than the emergence of coherent structure as a criterion for transition. The flow was perturbed by mean four jets in the fully developed section. It was stated that for the onset of turbulence, the maximum perturbed velocity equals 0.81 centerline velocity and that hairpin vortices exhibit instability and travel the entire channel height. Moreover, it was found that the minimal amplitude of disturbance scales as Re^{-1}, which is not in accord with the scaling of Chapman [22].

Liu and Gayme [103], introducing the structured input-output analysis which was adapted from the control theory, reproduced the results of Reddy et al. [87] simulations, showing that the initial oblique wave perturbations need less energy than the streamwise vortices perturbations to trigger the transition. Importantly, it was shown that the largest gain scales as $Re^{1.5}$ for the Reynolds number in the range of 500 to 4000 if the component-wise structure of nonlinearity is taken into account.

5. Plane Couette Flow

5.1. Phenomenology of Transition and Critical Reynolds Numbers

The mechanisms associated with traveling wave instability like the lift-up effect and the streak breakdown process (mentioned in subsection 3.1) can be seen in the plane Couette flow. In this subsection, the subcritical instability of the plane Couette flow, together with the different critical Reynolds numbers are discussed. It is noteworthy that Couette [104], measuring water viscosity in a thin gap between two coaxial vertical cylinders (with the outer cylinder rotating and the inner cylinder fixed), noticed that the transitional Re is roughly 480. In an experiment, Reichardt [105] found that the natural transition due to the finite amplitude disturbance happens at Re = 750.

Tillmark and Alfredsson [26] set up a laboratory apparatus to find the transitional Re for the plane Couette flow. The set-up consisted of a water channel with moving walls (transparent belts) in opposite directions. A drawback of the experiment was that the laminar velocity profile was not accessible for Re ≥ 400. However, inspecting the evolution of the turbulent spot revealed that the natural transition occurred at Re = 360±10. A fully turbulence state was achieved at Re ≈ 1000.

Daviaud et al. [106] experimentally found the critical Re for instability of Couette flows to be 370 ±10. They reported that the relaxation time of generated turbulent spots escalates when approaching the critical Re, i.e., they become self-sustaining for a long time.

In a rigorous work, Bergström [107] investigated the effects of the shape of the mean flow velocity profile on non-modal (i.e., transient) growth of 3-D initial disturbances in plane Couette-Poiseuille flows. The profile was in the form of $U(y) = A(1 - y^2) + By$. The mean flow with A = 0.5 and B = 1 gives the largest energy amplification for a streamwise-independent disturbance.

Recall that the plane Poiseuille flow is not linearly stable, but the plane Couette flow is. Klotz et al. [108] created an experimental setup to check the natural and forced instability of the Couette-Poiseuille flow. By numerically solving the Orr-Sommerfeld equation, they found that this flow turned unstable at Re = 10^8, whereas it showed instability at Re ≈ 480 and fully developed turbulence at Re = 780. Thus, they were the first to demonstrate that the transition of this type of flow is subcritical.

In another work, Klotz and Wesfreid [109] calculated the experimental transient growth of external disturbances in the plane Couette-Poiseuille flow. Accordingly, an initial period for formation the turbulent spots is required before the transient growth comes into play. They measured both mean and ensemble average energies. It was illustrated that the ensemble averaging underestimates the energy gain due to the instantaneous spanwise variation of the streaks.

Introducing the structured input-output analysis adapted from the control theory, Liu and Gayme [103] showed that the initial oblique wave perturbations need less energy than the perturbations by streamwise vortices to trigger the transition. Importantly, it was shown that the largest gain scales as $Re^{1.1}$ for the Reynolds number in the range of 300 to 4000 if the component-wise structure of nonlinearity is considered.

Liu and his coworkers [110] investigated the perturbation wavelengths in a stratified plane Couette flow using the structured input-output method. The velocity and the density gradients were considered inputs, and the nonlinear terms (i.e., forcing components) were considered outputs. Here, the Prandtl number (Pr) was the ratio of the kinematic viscosity to density diffusivity. It was realized that the well-established Miles-Howard criterion for stability (Ri_b ≤ 1/4, with Ri_b being the bulk Richardson number) corresponds to the most amplified perturbation when Pr = O(1).

Shuai et al. [111], using the structured input-output analysis and including the nonlinearity, studied the unstable plane Couette–Poiseuille flow. The velocity profile was written as $U(y) = \frac{3(1+\eta)}{4}(y^2 - 1) + \frac{1-\eta}{2}(y - 1) + 1$ where -1 ≤ y ≤ 1. Given that η characterizes the ratio of shear to driving pressure, the plane Couette flow (η = -1) is purely shear, the plane Poiseuille flow (η = 1) is purely pressure-driven, and η = 0 corresponds to the intermediate case. It was found that the highest perturbation gain (amplification) for η = 0 scales like $Re^{1.3}$. Figure 8 shows the scaling exponent for different values of η.

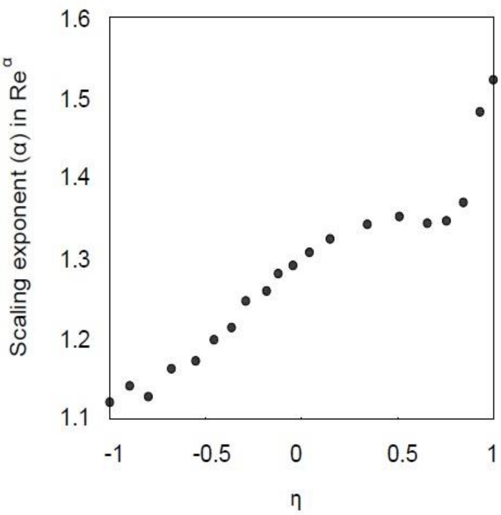

Fig. 8. The scaling exponent for the largest perturbation gain (amplification) vs. η for the plane Couette–Poiseuille flow (Shuai et al. [111]).

5.2. Scaling and Coherent Flow Structure

In this subsection, the scalings of perturbation amplitude for onset of instability in plane Couette flow, and a numerical coherent flow structure are mentioned. Again, it is emphasized that the coherent structures are signs of instability and transition to turbulence.

Lundbladh et al. [100] numerically examined the threshold amplitude for beginning the subcritical transition in plane Couette flows. It was found that the amplitude scales as $Re^{-5/4}$ for Reynolds number in the range of 500 to 2000.

Dauchot and Daviaud [112] experimentally examined the destabilization of plane Couette flow by finite amplitude perturbation. The experimental setup comprised two transparent walls moving in opposite directions with the same velocity and with the aid of two rotating cylinders. Due to limitations, the Reynolds number was less than 450. It was found that the critical perturbation amplitude scales like $A_c = O(Re\text{-}Re_{NL})^{-\alpha}$ where α is a constant and Re_{NL}=325 is the nonlinear global critical Reynolds number below which instability could not occur regardless of the perturbation amplitude.

Chapman [22] used asymptotic analysis (i.e., WKB theory) and showed that the amplitude of order Re^{-1} for both streamwise and oblique perturbations initiates transition in the plane Couette flow.

Floryan [113] analyzed the stability of a plane Couette flow under the wall transpiration. He noticed that the instability threshold amplitude varies as $Re^{-1.15}$ for high values of Reynolds number and 1% disturbances. Moreover, Re = 84 was established as the global threshold Reynolds number. Figure 9 shows the formation of streamwise vortices for Re = 5000 and S = 0.0015 at x = 3λ/4. Here, S is the amplitude of transpiration and λ stands for the wavelength of transpiration at the bottom wall.

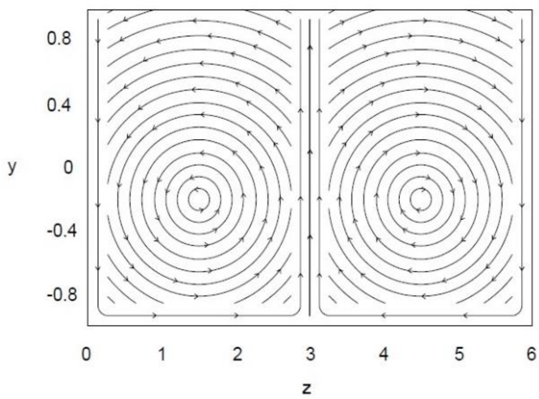

Fig. 9. Vector plot of perturbation velocities of plane Couette flow for Re = 5000 and S = 0.0015 at x = 3λ/4 with S being the transpiration amplitude and λ being the wavelength of wall transpiration (Floryan [113]).

Duguet et al. [114] performed a direct numerical simulation of the transition of the plane Couette flow spectrally. The Reynolds number ranges from 400 to 3500. They assessed the initial critical perturbation energy (E_c) vs Re for the streamwise vortices and oblique wave cases. They found that for both cases, $E_c = O(Re^{-2})$ conforming to the scaling of Chapman [22].

Duguet et al. [115] mapped out the subcritical transition by finite-amplitude perturbation in Couette flow by optimization. They proposed that the critical (i.e., least) perturbation kinetic energy for inducing transition is of $O(Re^{-2.7})$ for Re ≤ 3000. This scaling is comparable to that of pipe flow.

As mentioned before, Shuai et al. [111], using the structured input-output analysis and including the nonlinearity, studied the unstable plane Couette–Poiseuille flow. They stated that the threshold amplitude of perturbation to trigger instability for the plane Couette flow, plane Poiseuille flow, and the intermediate flow are $O(Re^{-1.1})$, $O(Re^{-1.5})$, and $O(Re^{-1.3})$, respectively.

The maximum allowable perturbation amplitude for natural transition (δ) is a small amplitude below which the flow state is laminar and above which the nonlinearity becomes prominent and the flow state is transitional. Hence, the amplitude greater than the maximum allowable perturbation amplitude is said to be of finite value. Some researchers studying the low-dimensional shear flow models like Joglekar et al. [116] using direct numerical simulation, Liu and Gayme [117], and Kalur et al. [118] using the input-output inspired analysis and formulating the nonlinear stability problem as linear matrix inequalities, tried to compute the maximum allowable amplitude. Joglekar et al. [116] proposed $\delta = 10^{2.61}Re^{-1.97}$ for 200 ≤ Re ≤ 2000. Most importantly, Floryan [113] reported the boundary between the small and finite amplitude perturbation. Accordingly, the average energy variations are significant as the value of perturbation amplitude becomes finite.

6. Conclusions and Recommendations

This paper reviewed the papers on the onset of transition to turbulence in parallel wall-bounded shear flows of Newtonian fluids, mainly in the last two decades. Furthermore, the important experimental and numerical results for the beginning of instability and natural transition were described. In addition, the different scalings of threshold amplitude of perturbation in terms of Reynolds number were mentioned. From the above review and discussions, the following conclusion can be drawn:

- Small-amplitude perturbations propagating in the flow can grow into finite-amplitude perturbations.
- The initial kinetic energy of small-amplitude disturbances grows much more than that of finite-amplitude ones (Sun and Hemati [96]).

- Traveling wave instability in pipe flow occurs at a high Reynolds number ($Re \to \infty$) for a long pipe, whereas it can occur at a finite Reynolds number for a moderate pipe length (Faisst and Eckhardt [39]).
- Hof et al. [44] experimentally observed and confirmed the traveling wave instability in the pipe flow. Since these traveling waves make the self-sustaining process (SSP) apparent, SSP is a reasonable route to turbulence for linearly stable flows.
- Tao [79] suggested an intriguing scaling for threshold roughness amplitude that initiates transition in pipe flow as $S = O(Re^{-2})$ where $S = n\varepsilon$ is the shape factor, ε is the roughness amplitude, and n is the axial wavenumber of the roughness.

Based on these results, the recommendations for future works are as follows:

- The scaling law of Chapman [22] for the onset of transition in plane Poiseuille flow was observed experimentally by Philip et al. [101]. Other experiments can be conducted to compare the scaling law of Chapman [22] for the onset of transition in plane Couette flow.
- Floryan and Floryan [93] compared the vortex instability against the traveling wave instability in a channel flow. Comparing these two types of instability in the pipe and plane Couette flows will be helpful for researchers.
- It is desirable to compare the scaling of small amplitude perturbation for the transition of developing flow with that of fully developed flow.
- Tao [79] illustrated a coherent structure in a rough-wall pipe flow composed of a pair of streamwise vortices with fast and slow streamwise streaks. Experimental visualization is needed to compare and contrast this theoretical finding.

Funding Statement

This research did not receive any specific grant from funding agencies in the public, commercial, or not-for-profit sectors.

Conflicts of Interest

The author declares that there is no conflict of interest or bias regarding the publication of this article.

References

[1] Eckert, M., 2021. Pipe flow: a gateway to turbulence. Arch. Hist. Exact Sci., 75, pp. 249–282.

[2] Ekman, V.W., 1911. On the change from steady to turbulent motion of liquids. Ark. Mat. Astron. Fys., 6(12), pp. 1–16.

[3] Pfenniger, W., 1961. Transition in the inlet length of tubes at high Reynolds numbers. In Boundary Layer and Flow Control (pp. 970–80), New York: Pergamon.

[4] Kundu, P.K. and Cohen, I.M., 2008. Fluid mechanics. 4th ed., Kidlington: Academic Press.

[5] Meseguer, A. and Trefethen, L.N., 2003. Linearized pipe flow to Reynolds number 10^7. J. Comput. Phys., 186 (1), pp. 178-197.

[6] John M.O., Obrist, D. and Kleiser, L., 2016. Secondary instability and subcritical transition of the leading-edge boundary layer. J. Fluid Mech., 792, pp. 682 – 711.

[7] Romanov, V.A., 1972. Stability of plane-parallel Couette flow. Funct. Anal. Applics., 7, pp. 137–146.

[8] Orszag, S. A., 1971. Accurate solution of the Orr-Sommerfeld stability equation. J. Fluid Mech., 50(4), pp. 689-703.

[9] Davey, A. and Drazin, P.G., 1969. The stability of Poiseuille flow in a pipe. J. Fluid Mech., 36, pp. 209-218.

[10] Herbert, T., 1976. Periodic Secondary Motions in a Plane channel. In Proceedings of the Fifth International Conference on Numerical Methods in Fluid Dynamics (pp. 235-240), Springer-Verlag, New York.

[11] Nishioka, M., S Iida, S. and Y.Ichikawa, Y., 1975. An experimental investigation of the stability of plane Poiseuille flow. J. Fluid Mech, 72, pp. 731-751.

[12] Patel, V.C. and Head, M.R., 1969. Some observations on skin friction and velocity profiles in fully developed pipe and channel flows. J. Fluid Mech. 38, pp. 181-201.

[13] Schmid, P.J. and Henningson, D.S., 2001. Stability and Transition in Shear Flows. New York: Springer.

[14] Serrin, J., 1959. Mathematical principles of classical fluid mechanics, In C. Truesdell (Eds.), Fluid Dynamics I/Strömungsmechanik I (pp. 125-263), Springer, Berlin, Heidelberg.

[15] Joseph, D.D. and Carmi, S., 1969. Stability of Poiseuille flow in pipes, annuli and channels, Q. Appl. Math., 26, pp. 575-599.

[16] Shahinpoor, M. and Ahmadi, G., 1972. Stability of Cosserat fluid motions. Arch. Rational Mech. Anal., 47, pp. 188-194.

[17] Ahmadi, G., 1976. Stability of a micropolar fluid layer heated from below. Int. J. Eng. Sci., 14(1), pp. 81-89.

[18] Mirzaee, H., Ahmadi, G., Rafee, R. and Talebi, F., 2023. Physical overview of the instability in laminar wall-bounded flows of viscoplastic and viscoelastic fluids at subcritical Reynolds numbers. Journal of Heat and Mass Transfer Research, 10(1), pp. 135-146.

[19] Yaglom, A. M., 2012. Hydrodynamic instability and transition to turbulence. Vol. 100. Dordrecht: Springer Science & Business Media.

[20] Manneville, P., 2016. Transition to turbulence in wall-bounded flows: Where do we stand?. Mech. Eng. Rev., 3(2), 15-00684.

[21] Kuwabara, S., 1967. Nonlinear instability of plane Couette flow. Phys. Fluids, 10(9), pp. S115-S116.

[22] Chapman, S.J., 2002. Subcritical transition in channel flows. J. Fluid Mech., 451, pp. 35-97.

[23] Davies, S.J. and White, C.M., 1928. An experimental study of the flow of water in pipes of rectangular section. Proceedings of the Royal Society of London, Series A, 119(781), pp. 92-107.

[24] Meksyn, D. and Stuart, J.T., 1951. Stability of viscous motion between parallel planes for finite disturbances. Proceedings of the Royal Society of London, Series A, 208(1095), pp. 517-526.

[25] Stuart, J.T., 1956. On the effects of the Reynolds stress on hydrodynamic stability. ZAMM-Journal of Applied Mathematics and Mechanics/Zeitschrift für Angewandte Mathematik und Mechanik, 36(S1), pp. S32-S38.

[26] Tillmark, N. and Alfredsson, P.H., 1992. Experiments on transition in plane Couette flow. J. Fluid Mech., 235, pp. 89-102.

[27] Böberg, L. and Brösa, U., 1988. Onset of Turbulence in a Pipe. Z. Naturforsch., 43a, pp. 697-726.

[28] Trefethen, L.N., Trefethen, A.E., Reddy, S.C. and Driscoll T.A., 1993. Hydrodynamic Stability without Eigenvalues. Science, 261 (5121), pp. 578-584.

[29] Landahl, M. T., 1972. Wave mechanics of breakdown. J. Fluid Mech., 56(4), pp. 775-802.

[30] Davidson, P. A., 2015. Turbulence: an introduction for scientists and engineers. 2nd ed., Oxford University Press.

[31] Hinze, J.O., 1975. Turbulence. 2nd ed., McGraw-Hill.

[32] Schmid, P.J. and Henningson, D.S., 1994. Optimal energy density growth in Hagen–Poiseuille flow. J. Fluid Mech., 277, pp. 197-225.

[33] Jovanović, M.R., 2021. From bypass transition to flow control and data-driven turbulence modeling: an input–output viewpoint. Annu. Rev. Fluid Mech., 53, pp. 311-345.

[34] Farrell, B.F. and Ioannou, P.J., 1993. Stochastic forcing of the linearized Navier–Stokes equations. Phys. Fluids, 5(11), pp. 2600-2609.

[35] Bamieh, B. and Dahleh, M., 2001. Energy amplification in channel flows with stochastic excitation. Phys. Fluids, 13(11), pp. 3258-3269.

[36] Darbyshire, A.G. and Mullin, T., 1995. Transition to turbulence in constant-mass-flux pipe flow. J. Fluid Mech, 289, pp. 83-114.

[37] Fedotov, S., Bashkirtseva, I. and Ryashko, L., 2002. Stochastic analysis of a non-normal dynamical system mimicking a laminar-to-turbulent subcritical transition. Phys. Rev. E, 66, p. 066310.

[38] Bergstrom, L.B., 2003. The effect of the Earth's rotation on the transient amplification of disturbances in pipe flow. Phys. Fluids, 15, pp. 3028-3035.

[39] Faisst, H. and Eckhardt, B., 2004. Travelling waves in pipe flow. Phys. Rev. Lett., 91, p. 224502.

[40] Wedin, H. and Kerswell, R.R., 2004. Exact coherent structures in pipe flow: travelling wave solutions. J. Fluid Mech., 508, pp. 333–371.

[41] Waleffe, F., 1997. On a self-sustaining process in shear flows. Phys. Fluids, 9(4), pp. 883-900.

[42] Hamilton, J.M., Kim, J. and Waleffe, F., 1995. Regeneration mechanisms of near-wall turbulence structures. J. Fluid Mech., 287, pp. 317-348.

[43] Waleffe, F., 1995. Hydrodynamic Stability and Turbulence: Beyond Transients to a Self-Sustaining Process. Studies in applied mathematics, 95(3), pp. 319-343.

[44] Hof, B., Van Doorne, C.W., Westerweel, J., Nieuwstadt, F.T., Faisst, H., Eckhardt, B., Wedin, H., Kerswell, R.R. and Waleffe, F., 2004. Experimental observation of nonlinear traveling waves in turbulent pipe flow. Science, 305(5690), pp. 1594-1598.

[45] Mellibovsky, F. and Meseguer, A., 2005. Global finite amplitude perturbations in medium aspect ratio pipe flow. J. Phys.: Conf. Ser., 14, p. 192.

[46] Mullin, T. and Peixinho, J., 2006. Recent Observations of the Transition to Turbulence in a Pipe. In Fluid Mechanics and Its Applications, vol. 78, (pp. 45-55), Springer, Dordrecht.

[47] Eckhardt, B., Schneider, T.M., Hof, B. and Westerweel, J., 2007. Turbulence Transition in Pipe Flow. Annu. Rev. Fluid Mech., 39, pp. 447–468.

[48] Nishi, M., Ünsal, B., Durst, F. and Biswas, G., 2008. Laminar-to-turbulent transition of pipe flows through puffs and slugs. J. Fluid Mech., 614, pp. 425–446.

[49] Loh, S.A. and Blackburn, H.M., 2011. Stability of steady flow through an axially corrugated pipe. Phys. Fluids, 23, p. 111703.

[50] Floryan, J. M., 2003. Vortex instability in a diverging–converging channel. J. Fluid Mech., 482, pp. 17-50.

[51] Tasaka, Y., Schneider, T.M. and Mullin, T., 2010. Folded Edge of Turbulence in a Pipe. Phys. Rev. Lett., 105, p. 174502.

[52] Avila, K., Moxey, D., De Lozar, A., Avila, M., Barkley, D. and Hof, B., 2011. The Onset of Turbulence in Pipe Flow. Sci., 333 (6039), pp. 192-196.

[53] Mullin, T., 2011. Experimental Studies of Transition to Turbulence in a Pipe. Annu. Rev. Fluid Mech., 43, pp. 1–24.

[54] Krauss, J., Ertunç, Ö., Ostwald, Lienhart, C.H. and Delgado, A., 2011. Evolution of transitional structures from puff to slug through multiple splitting in a pipe flow at low Reynolds number. J. Phys.: Conf. Ser., 318, p. 032012.

[55] Trip, R., Kuik, D.J., Westerweel, J. and Poelma, C., 2012. An experimental study of transitional pulsatile pipe flow. Phys. Fluids, 24, p. 014103.

[56] He, S. and Seddighi, M., 2013. Turbulence in transient channel flow. J. Fluid Mech., 715, pp. 60-102.

[57] Wu, X., Moin, P., Adrian, R.J. and Baltzerd, J.R., 2015. Osborne Reynolds pipe flow: Direct simulation from laminar through gradual transition to fully developed turbulence. PNAS, 112 (26), pp. 7920-7924.

[58] Hellström, L.H.O., Ganapathisubramani, B. and Smits, A.J., 2016. Coherent structures in transitional pipe flow. Phys. Rev. Fluids, 1, p. 024403.

[59] Novopashin, S.A., Skovorodko, P.A. and Sukhinin, G.I., 2016. Laminar-turbulent transition in Hagen–Poiseuille flow of a real gas. J. Turbl., 17 (9), pp. 870-877.

[60] Wu, X., Moin, P. and Adrian, R.J., 2020. Laminar to fully turbulent flow in a pipe: scalar patches, structural duality of turbulent spots and transitional overshoot. J. Fluid Mech., 896, A9.

[61] Cerbus, R.T. and Mullin, T., 2021. Driving determines the dynamics in transitional pipe flow. doi: 10.48550/arXiv.2110.14966.

[62] Zhou, Y., 2021. Turbulence theories and statistical closure approaches. Physics Reports, 935, pp. 1-117.

[63] Ricco, P. and Alvarenga, C., 2022. Growth of vortical disturbances entrained in the entrance region of a circular pipe. J. Fluid Mech., 932, A16.

[64] Hattori, H., Wada, A., Yamamoto, M., Yokoo, H., Yasunaga, K., Kanda, T. and Hattori, K., 2022. Experimental study of laminar-to-turbulent transition in pipe flow. Phys. Fluids 34, 034115.

[65] Avila, M., Barkley, D. and Hof, B., 2023. Transition to turbulence in pipe flow. Annu. Rev. Fluid Mech., 55, pp. 575-602.

[66] Panton, R.L., 2013. Incompressible Flow. 4th ed., John Wiley & Sons.

[67] Davidson, P.A., 2022. Incompressible fluid dynamics. Oxford University Press.

[68] Kline, S.J., Reynolds, W.C., Schraub, F.A. and Runstadler, P.W., 1967. The structure of turbulent boundary layers. J. Fluid Mech., 30(4), pp. 741-773.

[69] Hossain, M.Z. and Floryan, J.M., 2013. Instabilities of natural convection in a periodically heated layer. J. Fluid Mech., 733, pp. 33-67.

[70] Chandrasekhar, S., 1961. Hydrodynamic and hydromagnetic stability. Clarendon Press.

[71] Draad, A.A., Kuiken, G.D.C. and Nieuwstadt, F.T.M., 1998. Laminar–turbulent transition in pipe flow for Newtonian and non-Newtonian fluids. J. Fluid Mech., 377, pp. 267-312.

[72] Hof, B., Juel, A. and Mullin, T., 2003. Scaling of the turbulence transition threshold in a pipe. Phys. Rev. Lett., 91, p. 244502.

[73] Meseguer, A., 2003. Streak breakdown instability in pipe Poiseuille flow. Phys. Fluids, 15, pp. 1203-1213.

[74] Mellibovsky, F. and Meseguer, A., 2006. The role of streamwise perturbations in pipe flow transition. Phys. Fluids, 18, 074104.

[75] Ben-Dov, G. and Cohen, J., 2007. Instability of optimal non-axisymmetric base-flow deviations in pipe Poiseuille flow. J. Fluid Mech., 588, pp. 189–215.

[76] Peixinho, J. and Mullin, T., 2007. Finite-amplitude thresholds for transition in pipe flow. J. Fluid Mech., 582, pp. 169–178.

[77] Mellibovsky, F. and Meseguer, A., 2007. Pipe flow transition threshold following localized impulsive perturbations. Phys. Fluids, 19, 044102.

[78] Mellibovsky, F. and Meseguer, A., 2009. Critical threshold in pipe flow transition. Phil. Trans. R. Soc. A, 367, pp. 545–560.

[79] Tao, J., 2009. Critical instability and friction scaling of fluid flows through pipes with rough inner surfaces. Phys. rev. lett., 103(26), 264502.

[80] Nikuradse, J., 1933. Stromungsgesetze in Rauhen Rohren. VDI-Forschungsheft, 361.

[81] Schlichting, H. and Gersten, K., 2017. Boundary-Layer Theory. 9th ed., Berlin Heidelberg: Springer-Verlag.

[82] Colebrook, C. F., 1939. Turbulent flow in pipes, with particular reference to the transitional region between smooth and rough wall laws. J. Inst. Civil Engrs, 11, pp. 133–156.

[83] Cerbus, R.T., Sakakibara, J., Gioia G. and Chakraborty, P., 2020. The turbulent flow in a slug: a re-examination. J. Fluid Mech., 883, A13.

[84] Wygnanski, I. J. and Champagne, F. H., 1973. On transition in a pipe. Part 1. The origin of puffs and slugs and the flow in a turbulent slug. J. Fluid Mech., 59 (2), pp. 281–335.

[85] Ozcakir, O., Hall, P. and Blackburn, H.M., 2022. Exact coherent structures in pipe flow

in the presence of wall transpiration. J. Fluid Mech., 940, A41.

[86] Orszag, S.A. and Kells, L.C., 1980. Transition to turbulence in plane Poiseuille and plane Couette flow. J. Fluid Mech., 96(1), pp. 159-205.

[87] Reddy, S.C., Schmid, P.J., Baggett, J.S. and Henningson, D.S., 1998. On stability of streamwise streaks and transition thresholds in plane channel flows. J. Fluid Mech., 365, pp. 269 – 303.

[88] Jovanović, M.R. and Bamieh, B., 2005. Componentwise energy amplification in channel flows. J. Fluid Mech., 534, pp. 145-183.

[89] Biaua, D. and Bottaro, A., 2004. Transient growth and minimal defects: Two possible initial paths of transition to turbulence in plane shear flows. Phys. Fluids, 16, 3515.

[90] Schmid, P.J., Lundbladh, A. and Henningson, D.S., 1994. Spatial evolution of disturbances in plane Poiseuille flow. In Transition, Turbulence and Combustion: Volume I Transition (pp. 287-297), Kluwer, Dordrecht.

[91] Zienicke, E.A. and Krasnov, D., 2005. Parametric Study of the Streak Breakdown Mechanism in Hartman Flow. Phys. Fluids 17, 114101.

[92] Cohen, J., Philip, J. and Ben-Dov, G., 2009. Aspects of linear and nonlinear instabilities leading to transition in pipe and channel flows. Phil. Trans. R. Soc. A, 367, pp. 509–527.

[93] Floryan, J.M. and Floryan, C., 2009. Traveling wave instability in a diverging–converging channel. Fluid Dyn. Res., 42(2), p. 025509.

[94] Kaminski, A.K., Caulfield, C.P. and Taylor, J.R., 2017. Nonlinear evolution of linear optimal perturbations of strongly stratified shear layers. J. Fluid Mech., 825, pp. 213-244.

[95] Roy, P., Weisgraber, T.H. and Alder, B.J., 2017. The Onset of Turbulence in Wall-bounded Flows with Surface Roughness and Fluctuations. In Advances in the Computational Sciences, (pp. 52-66), World Scientific Publishing Co.

[96] Sun, Y. and Hemati, M., 2019. Suppressing subcritical transition in plane Poiseuille flow. In AIAA Aviation 2019 Forum, 3713, Dallas, Texas.

[97] Ren, J., Fu, S. and Pecnik, R., 2019. Linear instability of Poiseuille flows with highly non-ideal fluids. J. Fluid Mech., 859, pp. 89-125.

[98] Khan, H.H., Anwer, S.F., Hasan, N. and Sanghi, S., 2021. Laminar to turbulent transition in a finite length square duct subjected to inlet disturbance. Phys. Fluids, 33, 065128.

[99] Liu, C., Shuai, Y., Rath, A. and Gayme, D.F., 2023. A structured input-output approach to characterizing optimal perturbations in wall-bounded shear flows. doi: 10.48550/arXiv.2303.10498.

[100] Lundbladh, A., Henningson D.S. and Reddy, S.C., 1994. Threshold amplitudes for transition in channel flows. In Turbulence and Combustion (pp. 309-318), Kluwer, Dordrecht.

[101] Philip, J., Svizher, A. and Cohen, J., 2007. Scaling Law for a Subcritical Transition in Plane Poiseuille Flow. Phys. Rev. Lett., 98, 154502.

[102] Lemoult, G., Aider, J.L. and Wesfreid, J.E., 2012. Experimental scaling law for the sub-critical transition to turbulence in plane Poiseuille flow. Phys. Rev. E, 85, p. 025303(R).

[103] Liu, C. and Gayme, D.F., 2021. Structured input–output analysis of transitional wall-bounded flows. J. Fluid Mech., 927, A25.

[104] Couette, M., 1890. Etudes sur le frottement des liquides (Doctoral dissertation).

[105] Reichardt, H., 1956. Über die Geschwindigkeitsverteilung in einer geradlinigen turbulenten Couetteströmung. ZAMM-Journal of Applied Mathematics and Mechanics/Zeitschrift für Angewandte Mathematik und Mechanik, 36(S1), pp. S26-S29.

[106] Daviaud, F., Hegseth, J. and Bergé, P., 1992. Subcritical transition to turbulence in plane Couette flow. Phys. Rev. Lett., 69(17), p. 2511.

[107] Bergström, L.B., 2005. Nonmodal growth of three-dimensional disturbances on plane Couette–Poiseuille flows. Phys. Fluids, 17, 014105.

[108] Klotz, L., Lemoult, G., Frontczak, I., Tuckerman, L.S. and Wesfreid, J.E., 2017. Couette-Poiseuille flow experiment with zero mean advection velocity: Subcritical transition to turbulence. Phys. Rev. Fluids 2, 043904.

[109] Klotz, L. and Wesfreid, J.E., 2017. Experiments on transient growth of turbulent spots. J. Fluid Mech., 829, p. R4.

[110] Liu, C., Colm-cille, P.C. and Gayme, D.F., 2022. Structured input–output analysis of stably stratified plane Couette flow. J. Fluid Mech., 948, p. A10.

[111] Shuai, Y., Liu, C. and Gayme, D.F., 2023. Structured input–output analysis of oblique laminar–turbulent patterns in plane Couette–Poiseuille flow. Intl. J. Heat Fluid Flow, 103, p. 109207.

[112] Dauchot, O. and Daviaud, F., 1995. Finite amplitude perturbation and spots growth mechanism in plane Couette flow. Physics of Fluids, 7(2), pp. 335-343.

[113] Floryan, J.M., 2003. Wall-transpiration-induced instabilities in plane Couette flow. J. Fluid Mech. 488, pp. 151–188.

[114] Duguet, Y., Brandt, L. and Larsson, B.R.J., 2010. Towards minimal perturbations in transitional plane Couette flow. Physical Review E, 82(2), p. 026316.

[115] Duguet, Y., Monokrousos, A., Luca Brandt, L. and Henningson, D.S., 2013. Minimal transition thresholds in plane Couette flow. Phys. Fluids, 25, p. 084103.

[116] Joglekar, M., Feudel, U. and Yorke, J.A., 2015. Geometry of the edge of chaos in a low-dimensional turbulent shear flow model. Phys. Rev. E, 91(5), p. 052903.

[117] Liu, C. and Gayme, D.F., 2020. Input-output inspired method for permissible perturbation amplitude of transitional wall-bounded shear flows. Phys. Rev. E, 102(6), p. 063108.

[118] Kalur, A., Seiler, P. and Hemati, M.S., 2021. Nonlinear stability analysis of transitional flows using quadratic constraints. Phys. Rev. Fluids, 6(4), p. 044401.